Observation of kinetic Alfvén waves excited at substorm onset

N. Klöcker¹, H. Lühr¹, A. Korth² and P. Robert³

¹ Institut für Geophysik und Meteorologie der Technischen Universität Braunschweig, FRG

² Max-Planck-Institut für Aeronomie, Katlenburg-Lindau, FRG

³ Centre de Recherches en Physique de l'Environnement Terrestre et Planétaire, Issy-les-Moulineaux, France

Abstract. Ground-based observations of locally confined, very intense, drifting current systems by the EIS-CAT magnetometer cross in correlation with GEOS-2 measurements will be explained in terms of kinetic Alfvén waves. Particle and magnetic flux measurements on GEOS-2 indicate an excitation of the waves at the inner edge of the earthward-drifting plasma sheet by resonance mode conversion from hydromagnetic surface waves. The collapsing tail-like field configuration itself is identified as the surface wave. The comparison of theoretically deduced quantities with observational results reveals a satisfactory agreement between observations and theory.

Key words: Kinetic Alfvén waves – Resonance mode conversion – Expanding plasma sheet – Magneto-sphere-ionosphere coupling

Introduction

Recent ground observations of very intense magnetic pulsations with periods near the lower border of the Pi 2 frequency spectrum, in combination with riometer and STARE data, suggest the interpretation as ionospheric reflections of kinetic Alfvén waves. A detailed description of the event is published by Lühr et al. (1984) which will be referred to in the following as Paper 1.

The proof of kinetic Alfvén waves is of special interest in the actual discussion about high-latitude Pi 2 pulsations (Samson, 1982; Pashin et al., 1982; Baumjohann and Glaßmeier, 1984). Kinetic Alfvén waves are a special type of shear mode Alfvén waves, which always play an important role in the transmission of information along magnetic field lines. Shear mode Alfvén waves are generated by any change of the electric potential distribution in the magnetosphere-ionosphere system (i.e. any change in the magnetospheric convection pattern) and are always accompanied by field-aligned currents (Mallinckrodt and Carlson, 1978). The characteristic features of kinetic Alfvén waves are their large perpendicular wavenumber and their parallel elec-

Offprint requests to: N. Klöcker, Institut für Geophysik und Meteorologie der T.U. Braunschweig, Mandelssohnstr. 3, D-3300 Braunschweig, Federal Republic of Germany

tric field. Electrons can be accelerated by the electric field up to energies of a few keV. Narrow auroral structures and intense particle precipitation, which can be produced by these waves, are typical for the substorm breakup phase and Pi 2 pulsations, which occur in conjunction with breakup phenomena (see Samson, 1982 and references therein).

The propagation of shear mode Alfvén waves was theoretically studied by Fejer and Lee (1967) and Fejer and Kan (1969). On this basis and on Hasegawa's (1977) treatment of kinetic Alfvén waves, several attempts have been made to study the dynamics of coupling processes between the magnetosphere and the ionosphere. Goertz and Boswell (1979) analysed the effects of propagation and reflection of kinetic Alfvén waves at the ionosphere. Lysak and Carlson (1981) and Lysak and Dum (1983) extended this work by including the effect of turbulence, leading to a partial decoupling of the ionosphere from the magnetosphere. A possible source for kinetic Alfvén waves was provided by Hasegawa (1976) and further discussed by Goertz (1983). Hasegawa has shown that a large-scale incompressible MHD surface wave can be converted to small-scale Alfvén waves.

During the first mentioned pulsation event the European Geostationary Satellite GEOS-2 was in a position magnetically conjugate to the EISCAT magnetometer chain (Paper 1). Particle and magnetic field fluctuations measured on GEOS in conjunction with the ground-based observations will be presented in this paper. They can satisfactorily be explained in terms of the theoretical frame outlined by Hasegawa (1976) and Goertz (1983). At first the GEOS-2 observations will be introduced followed by a detailed comparison of observed and theoretically deduced parameters.

Observations on GEOS-2

Energetic particle flux

On the day of interest – 2 November 1982 – the geostationary satellite GEOS-2 was located at a geographic longitude of 32.2°E and a geomagnetic latitude of about 3°S.

The particle measurements onboard GEOS-2 were made with the MPAe charged-particle spectrometer (Korth and Wilken, 1978; Korth et al., 1978) which

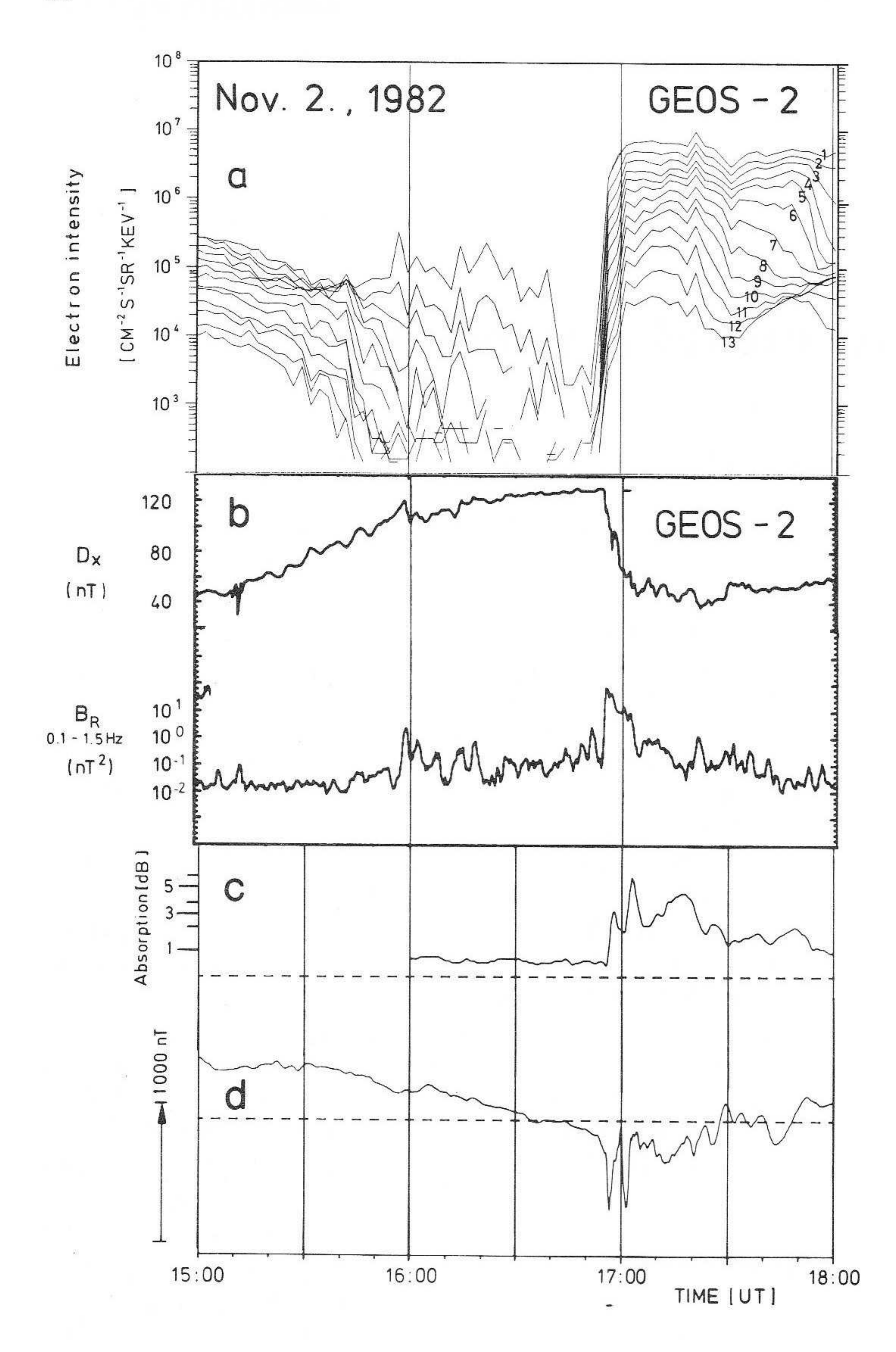


Fig. 1a-d. Synchronous observations made onboard the geostationary satellite GEOS-2 and on ground in northern Scandinavia in the same local time sector.

- a Differential electron intensities in 13 energy channels. The data were averaged over 2.5 min. The band widths in keV of the different labelled channels are as follows: 1: 24–30; 2: 30–38; 3: 38–45; 4: 45–52; 5: 52–61; 6: 61–71; 7: 71–83; 8: 83–96; 9: 96–114; 10: 114–133; 11: 133–154; 12: 154–180; 13: 180–214. Around 1710 UT these channels can be identified in the given sequence with the highest intensity for the lowest energy band.
- b The equatorial component of the magnetic field D_x measured on board GEOS-2 with the search coil magnetometer and the integrated power in the ULF range from 0.1-1.5 Hz in B_R , the right-handed polarized component in the equatorial plane.
- c and d Ground-based observations of the cosmic radio noise absorption at the Finnish station Rovaniemi (c), indicating an unusual enhancement of the ionospheric plasma density at 1656 UT, and the geographic north component of the EISCAT magnetometer station Muonio (d). Simultaneously with the onset of the very strong

Simultaneously with the onset of the very strong magnetic pulsation, all other observations show rapid variations

detected ions and electrons. For this study only electron data are shown. Electrons were measured simultaneously at energies > 22 keV as well as in 13 energy channels between 24 and 213 keV.

The electron intensities in the 13 energy channels are presented in Fig. 1a. The electrons were detected perpendicular $(90^{\circ}\pm5^{\circ})$ to the S/C spin axis (pitch angle calculations could not be carried out because the fluxgate magnetometer failed in 1979). From 1500 UT we observe a steady decrease of the intensities in all energy channels. At 1654 UT a sudden energy dispersionless increase by 2–3 orders of magnitude is recorded. About 10 min later the maximum intensity is reached.

The decrease in the electron intensity can be explained by a change in the local magnetic field topology at geostationary orbit. From Fig. 1b it can be demonstrated that after 1500 UT the magnetic field (measured by the search coil magnetometer) becomes more and more tail-like until substorm onset at 1654 UT. The onset is associated with a strong injection of energetic electrons and ions (Fig. 2) at the geostationary orbit and with a rapid return to a dipole-like magnetic field configuration. This behaviour is well

known from the work of Baker and co-workers (e.g. Baker et al., 1982). In addition, Fig. 3 shows count rates of electrons with energies > 22 keV for a longer time period than in Fig. 2. Fluctuations in the period range between 250 and 500 s can clearly be identified.

Magnetic flux variations

Figure 1 b shows the equatorial projection D_x of the magnetic field and the integrated power in the frequency range 0.1-1.5 Hz in B_R , the right-handed polarized component in the equatorial plane. The ULF fluxmeter and the deconvolution method used to obtain an equivalent de magnetic measurement are described by Robert et al. (1984). Around 1500 UT the increasing D_{x} indicates a developing tail-like magnetic field configuration in the same way as discussed by Shepherd et al. (1980) and Baker et al. (1982). During this time GEOS-2 entered the nightside magnetosphere where, during the growth phase of a substorm, cross-tail currents have often been observed in the near earth region. At 1654 UT this configuration starts collapsing, lasting until 1703 UT when the undisturbed dipolar configuration was reached again. The additional field value in this

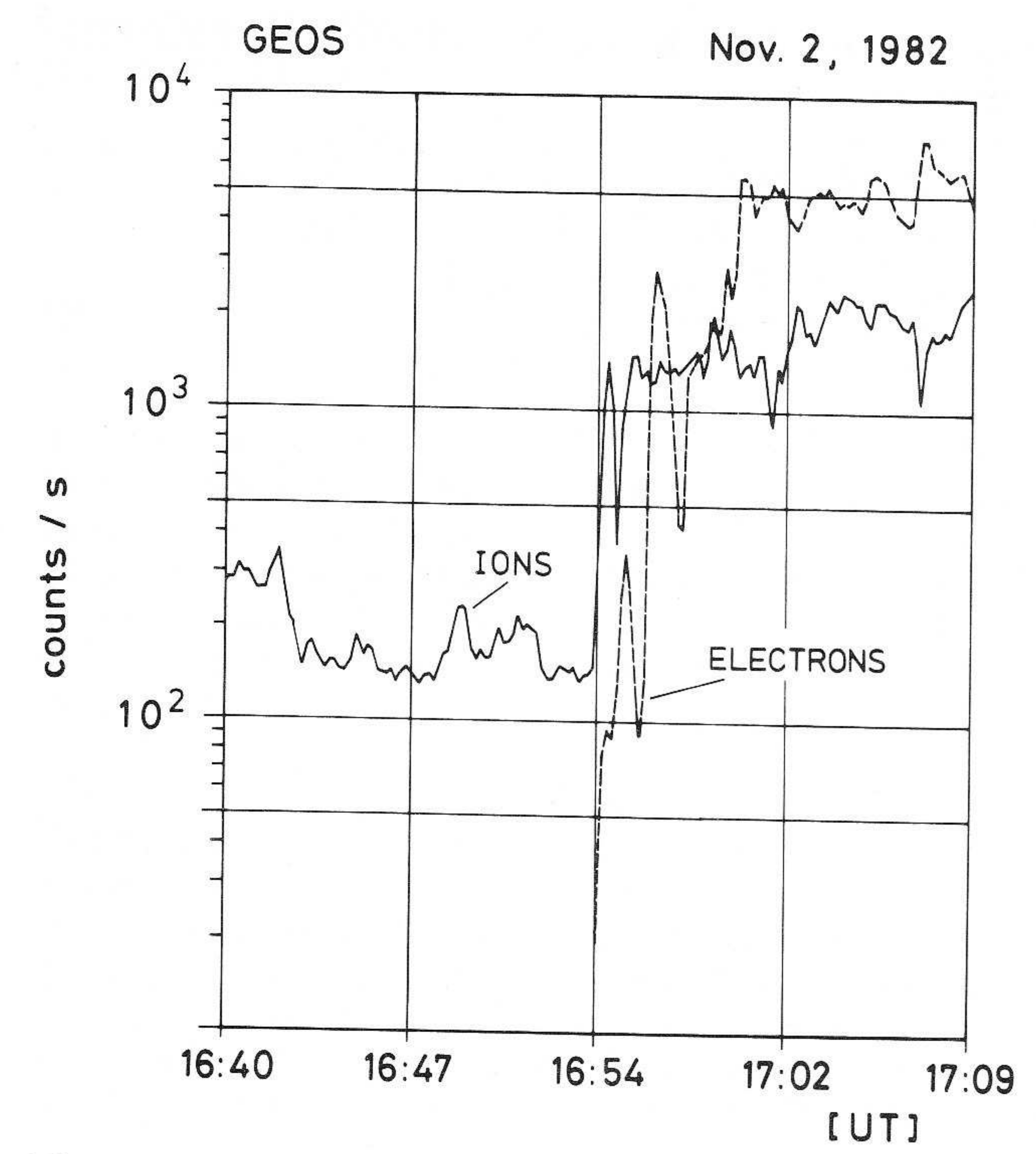


Fig. 2. This shows the detected electrons as well as the ions in the spin plane of GEOS-2 integrated over all energy channels, i.e. from 24 to 214 keV for the electrons and from 35 to 403 keV for the ions. The data were averaged over 11 s yielding a much better time resolution than in Fig. 1a. The rise time for ions is about 30 s. The electrons increase stepwise with peak intensities after 75 s, 150 s, and 350 s

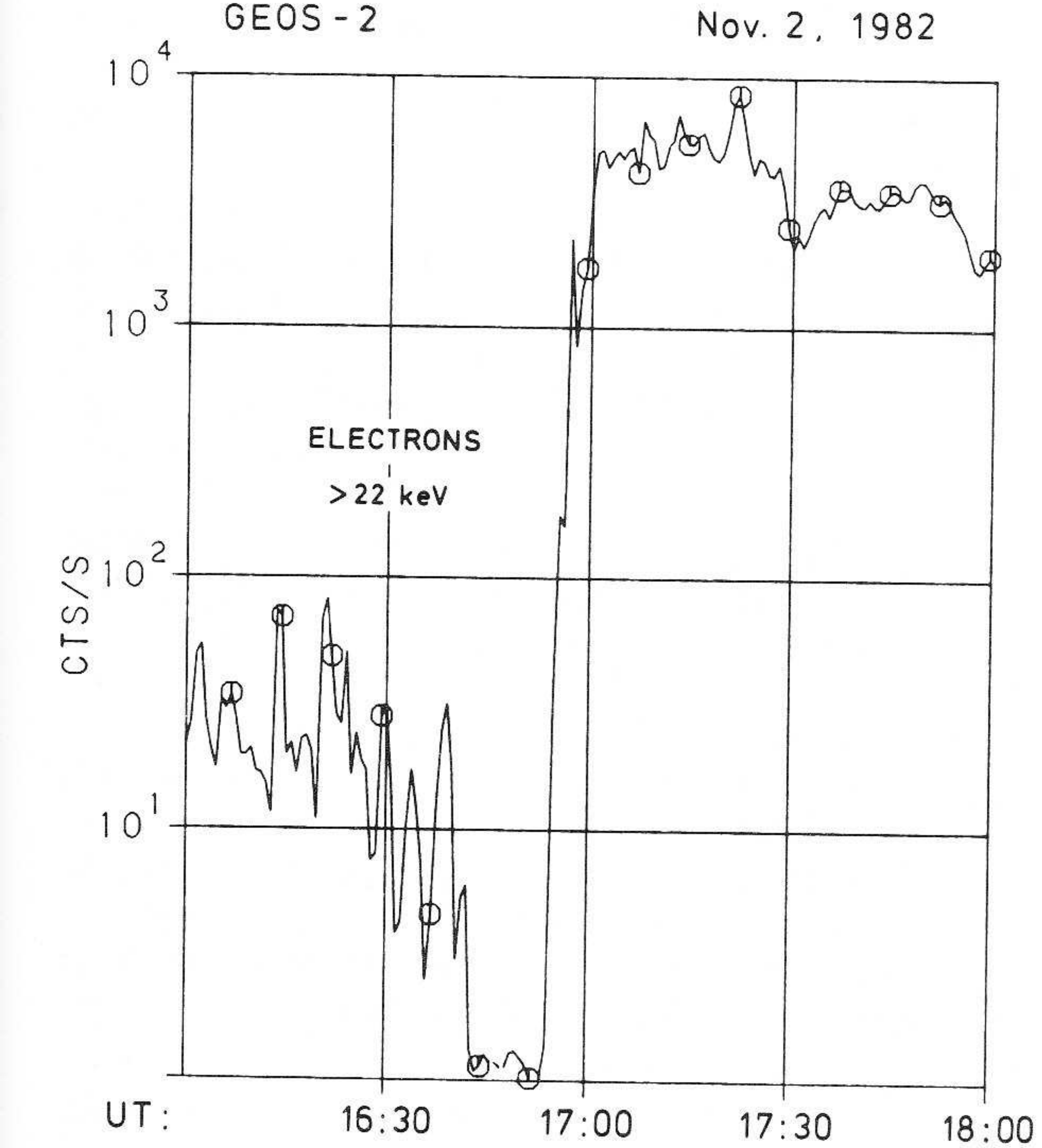


Fig. 3. Count rates of electrons in the spin plane integrated above an energy level of 22 keV. The data were averaged over 45 s. Pulsations in the period range 250-500 s before and after substorm onset are present

component amounted to $80\,nT$. At the beginning of the collapse the field changed by $-0.2\,nT/s$.

During the transition from a tail-like towards a dipolar configuration, strong ULF emissions with short irregular pulsations (SIPs) occurred which are typical of the substorm onset (Shepherd et al., 1980). The SIPs are interpreted by Robert et al. (1984) as the signature of current structures parallel to the magnetic field passing by the spacecraft with a high velocity. In their analysis they obtain an average drift velocity of $70 \, \mathrm{km/s}$, an average current density of $8 \times 10^{-8} \, \mathrm{A/m^2}$ and an average dimension of $200 \, \mathrm{km}$. In our case, pulsations are observed in the D_x component with a period of $265 \pm 60 \, \mathrm{s}$ (Fig. 1b).

For completeness, *E*-field measurements would be highly desirable. Unfortunately, the electron beam experiment on GEOS-2 failed around June 1979 and since the data received from the electric field experiment (Pedersen et al., 1978) need such serious corrections due to photo-electrons and the wake effect (O. Bauer, personal communication), we decided not to include them.

Summary of ground observations

Figure 1 shows the simultaneously recorded ground observations of the cosmic radio noise absorption (Fig. 1c) at the station Rovaniemi and the geographic north component of the magnetic field at Muonio (Fig. 1d). A detailed description of these observations is contained in Paper 1. For completeness, the main characteristics are listed in the following:

- The amplitudes of the magnetic pulsations reached values of up to 1000 nT in the horizontal component.
- The period of the pulsations was $340 \pm 50 \,\mathrm{s}$.
- The magnetic perturbations on the ground originated from almost two-dimensional ionospheric current systems with a width of the order of 20 km.
- The current bands drifted like parallel wavefronts in a southwest direction with a velocity $v_d = 2.3 \pm 0.3$ km/s. They have been observed down to latitudes corresponding to L < 3.3.
- The distance between the wavefronts was more than a factor 10 larger than the width of the current bands, so that the magnetic perturbations could be observed on the ground.
- There was a nearly one-to-one correspondence between the drifting wavefronts and the locally confined enhancement in ionization.
- The simultaneous onset of a substorm was indicated by mid-latitude Pi 2 activity.
- The current bands we observed were on the poleward side of the well-developed Harang discontinuity.

Excitation of kinetic Alfvén waves

A theory by which most of the observed features can be explained coherently has been provided by Hasegawa (1976) and was further discussed by Goertz (1983). This theory combines the creation of narrow structures like auroral arcs and small-scale ionospheric current bands by kinetic Alfvén waves with the possible

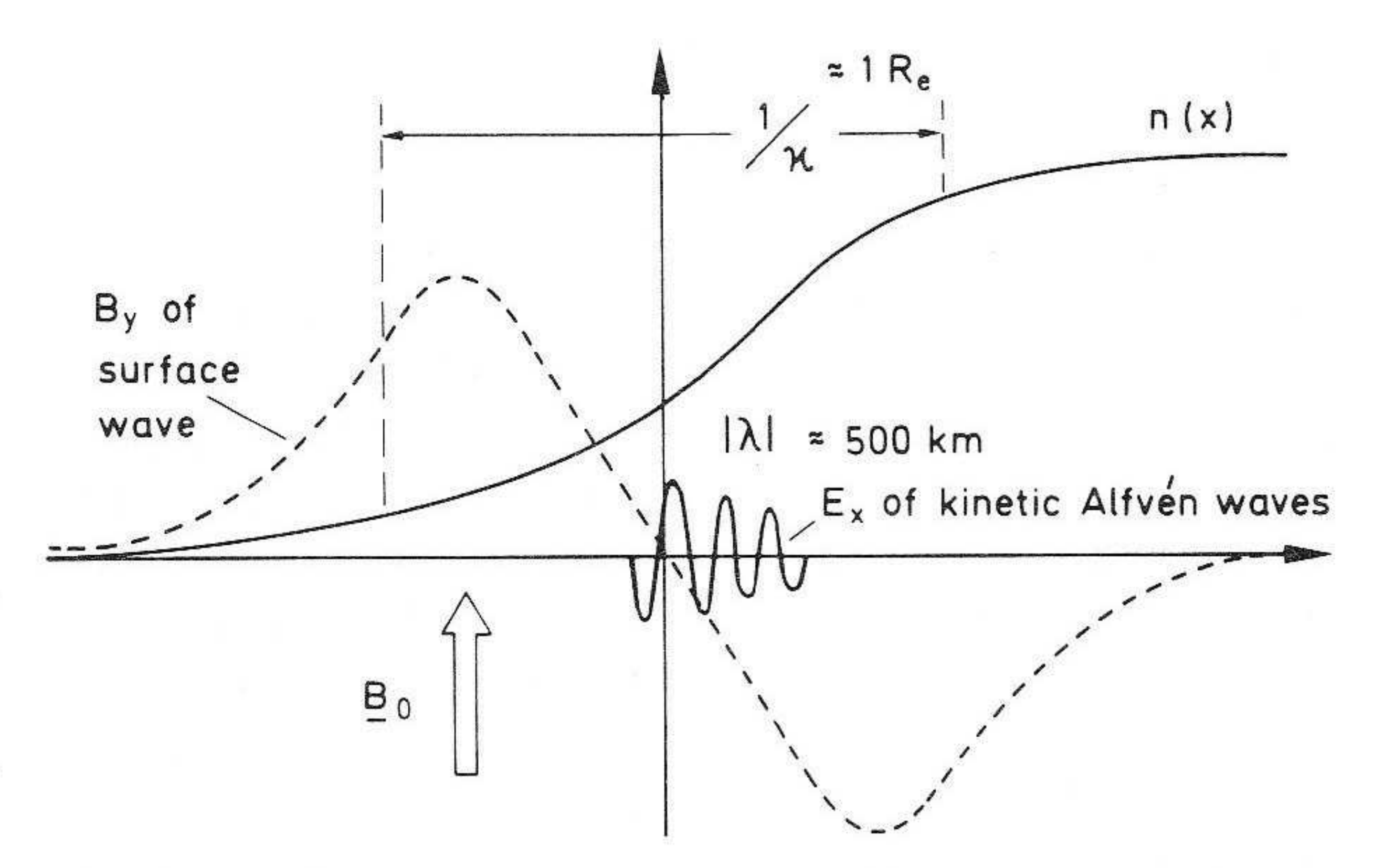


Fig. 4. Profile of the surface wave, the density variation and the kinetic Alfvén wave (after Hasegawa, 1976)

source of these waves in the magnetosphere. The basic mechanism is the resonant mode conversion of large-scale MHD surface waves to kinetic Alfvén waves.

At boundaries within the magnetosphere like the plasmapause, the inner edge of the plasma sheet and the plasma sheet boundary layer, surface waves can be excited by macroscopic MHD instabilities, e.g. the Kelvin-Helmholtz instability. The dispersion relation for a surface wave along the plasma-vacuum interface is given by (Hasegawa, 1976):

$$\omega_s = \sqrt{2} k_{\parallel} v_A$$

where $v_A = B_0/\sqrt{\mu_0 n_i m_i}$ is the Alfvén velocity and k_{\parallel} is the wavenumber parallel to the ambient magnetic field. The index s denotes surface wave parameters.

If the plasma density varies smoothly between zero at $x \to -\infty$ and n_0 at $x \to \infty$ (Fig. 4) the eigenmode of local shear Alfvén waves can be in resonance with the surface wave and, therefore, can extract energy from the surface wave. The coupling occurs where the local Alfvén velocity $v_A(x)$ is equal to $\sqrt{2}v_A(x \to \infty)$.

The sharp density gradient in the keV electrons and ions (Fig. 2) observed on GEOS is regarded as the inner edge of the expanding plasma sheet. The ratio of magnetic to kinetic energy density β is of the order of $0.3 \gg m_e/m_i$. We are therefore dealing with the warm plasma case. Then the ion gyroradius ρ_i becomes a critical length for small-scale perturbations. Under simplified conditions, i.e. the plasma density is taken locally constant, near the resonance point the dispersion relation of the Alfvén waves has the form [Hasegawa, 1976; Eq. (23)]:

$$\omega^2 = k_{\parallel}^2 v_A^2 (1 + k_x^2 \rho^2); \tag{1}$$

with

$$\rho^2 = \left(\frac{3}{4} + \frac{T_e}{T_i}\right) \rho_i^2. \tag{2}$$

This expression implies a propagation of the wave across the ambient magnetic field. (T_e , T_i are the temperatures of the electron and ion gas, respectively, and ρ_i is the ion gyroradius.)

The solution of the wave equation for the perpen-

dicular electric field derived by Hasegawa [his Eq. (31)] is given by

$$E_{x} = -\frac{\pi^{1/2} E_{0}}{(\kappa \overline{\rho})^{2/3}} \left(\frac{\delta}{x}\right)^{1/4} \exp\left\{i \left[\frac{2}{3} \left(\frac{x}{\delta}\right)^{3/2} + \frac{\pi}{4}\right]\right\}$$

$$+\frac{E_{0}}{\kappa x} \quad \text{for } x > 0.$$

$$(3)$$

In this equation E_0 is the amplitude of the surface electric wave, κ is the inverse scale length of the plasma gradient, which is taken to be linear. $\bar{\rho}$ is similar to ρ in Eq. (2), but differs by a factor multiplied to the temperature ratio. This factor has a value between 0 and 1 depending on the plasma density fraction $n(x)/n(x\to\infty)$ at the resonance point. $\delta = (\bar{\rho}^2/\kappa)^{1/3}$ is also a scale length.

The first term in Eq. (3) represents the kinetic Alfvén wave and the second term the MHD surface wave. The wave equation solution for the low-density side of the surface (x < 0) contains only the surface wave, i.e. under given conditions of a warm plasma the Alfvén wave propagates only into the higher-density side of the resonance point. The perpendicular wavelength of the kinetic Alfvén wave is given by the exponent of Eq. (3)

$$\lambda_x = 0.7 \,\delta. \tag{4}$$

A sketch of the spatial distribution of the plasma density, the surface wave fields and E_x of the kinetic Alfvén wave is shown in Fig. 4.

The amplitude E_x of the kinetic Alfvén wave near the resonance point can be expressed in terms of the y component of the surface wave magnetic field B_{sy} if we replace E_0 in Eq. (3) by $v_A B_{sy}$ and consider the region where $\kappa \cdot x$ is of the order 1. Then we get

$$|E_x| = \frac{v_A}{\sqrt{\kappa \rho}} B_{sy}, \tag{5}$$

and hence the magnitude of the perpendicular potential drop ϕ becomes

$$|\phi| = \frac{1}{k_x} \frac{v_A}{\sqrt{\kappa \rho}} B_{sy}. \tag{6}$$

Goertz (1983) derived the ratio of the parallel potential drop ψ to ϕ in the case of warm plasma

(1)
$$\frac{\psi}{\phi} \approx 2 \left[\kappa \rho_i \cdot \frac{\left(\frac{T_e}{T_i}\right)^3}{\left(\frac{3}{4} + \frac{T_e}{T_i}\right)} \right]^{2/3}. \tag{7}$$

Finally, the equation for the parallel current density j_z , given by Hasegawa (1976), has the form

$$j_z = \frac{k_x}{\mu_0} \frac{T_i}{T_e} \frac{B_{sy}}{\sqrt{\kappa \rho_i}}.$$
 (8)

The results from these equations will now be confronted with observational results.

Comparison of observational and theoretical results

First of all we have to identify the MHD surface wave to which the Alfvén waves can couple and which can provide enough energy. The properties of the surface wave are not too restricted by the theory. Hasegawa (1976) has emphasized that the coupling does not depend on the frequency of the surface wave. We only have to look for a large-scale $\partial B/\partial t$. This is given by the reconfiguration of the dipole field occurring simultaneously with the crossing of the plasma sheet boundary.

The excess magnetic field energy near the inner edge of the plasma sheet, which has partly been converted to kinetic Alfvén waves, can be estimated by the equation

$$E_B = d_{\perp} \cdot d_{\parallel} \frac{(\Delta B)^2}{2 \mu_0}.$$

 E_B is magnetic energy per length along the plasma sheet boundary. d_{\perp} is the thickness of the boundary in x taken roughly as $1R_e$ (earth radius), which can be considered as a lower limit derived from the decrease in D_x (Fig. 1b), and an assumed drift velocity of the convecting plasma sheet of about $70\,\mathrm{km/s}$. d_{\parallel} is the extent of the tail-like field configuration perpendicular to the equatorial plane. With $d_{\parallel} \approx 5R_e$ and $\Delta B = 80\,\mathrm{nT}$ we get:

$$E_B \approx 5 \times 10^5 \,\mathrm{J/m}$$
.

This value has to be compared with the energy density of the excited waves.

For mode conversion we have to consider the y component of the large-scale magnetic field perturbation. This component is generated either by the crosstail currents themselves which are responsible for the tail-like field distortion or by the field-aligned currents in the plasma sheet boundary layer, by which the interrupted equatorial currents are closed via the ionosphere. In both cases we have to take the field component along the plasma sheet boundary. For the following computations we assume $B_{sy} = 10 \, \mathrm{nT}$, which seems to be a conservative estimate.

The temperatures T_e , T_i are taken to be equal, hence we get $\rho = 1.3 \, \rho_i$ in Eq. (2). The uncertainties in the actual values justify the assumption $\bar{\rho} \approx \rho_i$. A 20-keV proton has a $\rho_i \approx 200 \, \mathrm{km}$ in a magnetic field of flux density $B = 100 \, \mathrm{nT}$.

For the estimation of the scale length $1/\kappa$ of the plasma gradient we need the earthward-directed drift velocity of the expanding plasma sheet. On the ground we have observed equatorward-directed velocities around 2.3 km/s. Projected on the equatorial plane, taking into account the divergence of the field lines in the meridional plane by a factor of 30 for a L=6.6 field line, we get $v_d=70\,\mathrm{km/s}$. Together with the rise time of the warm plasma density on GEOS (see Fig. 2) of about 30 s for the ions and 130 s for the stepwise increasing electron flux, we achieve a scale length $1/\kappa=1R_e$ as a mean value $(1/\kappa=0.3\,R_e)$, if we regard only the warm ions). Hence from Eq. (4) we get the perpendicular wavelength of the kinetic Alfvén wave in the equatorial plane, $\lambda_r \approx 430\,\mathrm{km}$ ($\approx 300\,\mathrm{km}$). If we project

these values down along the field lines, we have

$$\lambda_{\rm x} \approx 15 \,\rm km \ (\approx 10 \,\rm km)$$

at the ionospheric altitude. This is in good agreement with the observational result of 20 km for the width of the ionospheric current band.

Next we compare the amplitude of the wave electric field, given by Eq. (5), with our observations. With the above values for κ , ρ and B_{sy} , and taking $v_A = 1,000\,\mathrm{km/s}$, as a typical value for the equatorial plane, we get $|E_x| \approx 60\,\mathrm{mV/m}$ near the source region of the Alfvén waves. Fields of this order of magnitude have been published by Aggson et al. (1983). Again, projected down to the ionospheric level, the electric field of the downward-travelling Alfvén wave has an amplitude

$$E_x \approx 1.8 \text{ V/m}.$$

From ground observations we deduced $E_x \approx 2 \text{ V/m}$ (see Paper 1). The potential ϕ is then easily computed in accordance with Eq. (6) by multiplying E_x with $\lambda_x/2\pi = 1/k_x \approx 3 \times 10^3 \text{ m}$:

$$\phi \approx 5 \,\mathrm{kV}$$
.

And hence, from Eq. (7), we have for the parallel potential drop over the wavelength of the guided Alfvén waves

$$\psi \approx 1 \,\mathrm{kV}$$
.

The surface wave, which is mode converted to the kinetic Alfvén wave, does not change in time harmonically but varies with nearly constant $\partial B/\partial t$. For an observer moving with the inner edge of the plasma sheet nothing happens in time. For this reason, trapping by the wave and direct acceleration by the parallel potential may account for the energization and precipitation of electrons. The estimated value of ψ is somewhat small but of the right order of magnitude. Typical energy values for auroral electrons are between 2 and 3 keV.

Landau damping may also be considered as a possible wave-particle interaction for electrons which move with nearly the phase velocity of the Alfvén wave. Since v_A grows from about 1,000 km/s near the equator up to a maximum of $10000 \, \mathrm{km/s}$ at a height of $1-2\,R_e$, thermal electrons can be accelerated up to a few ten keV. The efficiency of this mechanism depends on the fraction of resonant electrons in the plasma sheet and a detrapping of the electrons when the wave approaches the ionosphere with decreasing phase speed.

The field-aligned current density associated with the kinetic Alfvén wave can be estimated by Eq. (8). Near the equator we obtain $j_z \approx 0.6 \,\mu\text{A/m}^2$. At the ionospheric altitude the projected value comes out as

$$j_z \approx 200 \,\mu\text{A/m}^2$$
.

This agrees with the observational result.

Finally, we compare the energy carried by the kinetic Alfvén wave with the released magnetic energy E_B . The integrated energy flux per length along the wavefront is approximately given by:

$$E_{w} = \lambda_{x} \Delta t \frac{E_{\perp}^{2}}{v_{A} \mu_{0}}.$$

 Δt is the time period of the wave to travel along the ambient magnetic field over one wavelength. $\Delta t = \lambda_z/v_A$ $=\lambda_x/v_d \approx 10 \text{ s. We obtain}$

$$E_w \approx 1.5 \times 10^4 \,\mathrm{J/m}$$

near the equatorial plane. Hence the wave energy in a wavefront in one hemisphere makes up 3 % of the total available free magnetic energy.

Discussion

The agreement between observational and theoretical results is striking. It is even so good that one may forget the estimative character of the theoretical quantities. Therefore, we wish to point out that only the order of magnitude of the quantities is relevant for their comparison.

The good agreement confirms our opinion that the pulsation event of 2 November 1982 can be explained in terms of kinetic Alfvén waves generated along the inner edge of the plasma sheet. This explanation is also supported by the fact that the pulsation occurred only on the poleward side of the plasma sheet boundary layer (see Paper 1). According to Eq. (3), the kinetic Alfvén waves propagate into the dense region when the warm plasma case applies. The observed drift velocity on ground then results from the difference between the earthward-directed drift of the warm plasma sheet plasma and the roughly oppositely directed propagation of the kinetic Alfvén waves. The direction of the drift velocity on the ground is determined by the relative magnitude of both velocities concerned. For similar events during that winter (not discussed here), poleward-directed drifts of the wavefronts have also been observed.

After the studies of Lysak and Carlson (1981) and Lysak and Dum (1983) the question arises whether our interpretation of the observations may be in conflict with their theoretical results, i.e. that damping processes must be taken into account. They would cause a reflection of the Alfvén waves at heights above the ionosphere. Up to an altitude of about $4R_e$, where the cold plasma approximation is valid, kinetic Alfvén waves can be affected by anomalous resistivity due to microscopic turbulences (Lysak and Carlson, 1981). The turbulence is generated when the drift velocity, v_D $=j_z/ne$, exceeds v_c , the critical drift for instability. Hence, the reflection of Alfvén waves at turbulent regions in the model of Lysak and Dum (1983) becomes more effective with increasing current or decreasing scale size. At altitudes around $6,000 \,\mathrm{km}$ where v_D reaches its maximum, we get, for a plasma density n=5 $\times 10^7 \,\mathrm{m}^{-3}$ and $j_z = 30 \,\mu \text{A/m}^2$, $v_D \approx 4{,}000 \,\mathrm{km/s}$. For T_i = 100 eV we have $v_c \approx 2,000 \, \mathrm{km/s}$. These calculated values do not allow a clear decision as to whether we have to expect a partial decoupling of the ionosphere from the magnetosphere or not. In situ measurements in this region would allow for more precise statements. The existence of a turbulent region would also cause a broadening of the wavefront by a factor of two or

more. But this effect is too small to lead to significant

discrepancies in our comparison.

In the same altitude region wave energy can be converted to particle energy by Landau damping (Fejer and Kan, 1969; Klöcker, 1982). For this wave-particle interaction a sufficient amount of resonating electrons has to be present in the magnetic flux tube. The resonant growth rate also depends on the scale size of the Alfvén waves perpendicular to the magnetic field. The existence of precipitated electrons during the event of 2 November can be interpreted as an indication for such a coupling process. But for final conclusions we would need more information, such as the spectral energy distribution of the auroral electrons.

The next step in this study of kinetic Alfvén waves will be to look for more pulsation events in the evening sector occurring concurrently with the onset of substorms in order to identify general characteristics of these phenomena and in order to get more reliable

quantities for a comparison with theory.

Acknowledgements. We thank Dr. H. and A. Ranta from Sodankylä Geophysical Observatory for providing the riometer recording. The EISCAT Magnetometer Cross is a joint enterprise of the Finnish Meteorological Institute, the Geophysical Observatory of Sodankylä and the Technical University of Braunschweig. The German part has been funded by grants of the Deutsche Forschungsgemeinschaft.

References

Aggson, T.L., Heppner, J.P., Maynard, N.C.: Observations of large magnetospheric electric fields during the onset phase of a substorm. J. Geophys. Res. 88, 3981-3990, 1983

Baker, D.N., Hones, jr., E.W., Belian, R.D., Higbie, P.R., Lepping, R.P., Stauning, P.: Multiple-spacecraft and correlated riometer study of magnetospheric substorm phenomena. J. Geophys. Res. 87, 6121-6136, 1982

Baumjohann, W., Glaßmeier, K.-H.: The transient response mechanism and Pi 2 pulsations at substorm onset. Planet.

Space Sci. 31, 1984 (in press)

Fejer, J.A., Kan, J.R.: A guiding centre Vlasov equation and its application to Alfvén waves. J. Plasma Phys. 3, 331-351, 1969

Fejer, J.A., Lee, K.F.: Guided propagation of Alfvén waves in the magnetosphere. J. Plasma Phys. 1, 387-406, 1967

Goertz, C.K.: Nonstationary coupling between the magnetosphere and ionosphere. Sixth ESA-Sympos. European rocket balloon programme. (ESA SP-183), 221-228, 1983

Goertz, C.K., Boswell, R.W.: Magnetosphere-ionosphere coupling. J. Geophys. Res. 84, 7239-7246, 1979

Hasegawa, A.: Particle acceleration by MHD surface wave and formation of aurora. J. Geophys. Res. 81, 5083-5090, 1976

Hasegawa, A.: Kinetic properties of Alfvén waves. Proc. Indian Acad. Sci. 86A, 151-174, 1977

Klöcker, N.: Observation of guided ULF-waves correlated with auroral particle precipitation theoretically explained by negative Landau damping. J. Geophys. 51, 119-128, 1982

Korth, A., Wilken, B.: New magnetic electron spectrometer with directional sensitivity for a satellite application. Rev. Sci. Instrum. 49, 1435-1440, 1978

Korth, A., Kremser, G., Wilken, B.: Observations of substorm associated particle-flux variations at $6 \le L \le 8$ with GEOS-1. Space Sci. Rev. 22, 501-509, 1978

Lühr, H., Klöcker, N., Thürey, S.: Ground-based observations

of a very intense substorm-related pulsation event. J. Geophys. 55, 41–53, 1984

Lysak, R.L., Carlson, C.W.: The effect of microscopic turbulence on magnetosphere-ionosphere coupling. Geophys. Res. Lett. 8, 269–272, 1981

Lysak, R.L., Dum, C.T.: Dynamics of magnetosphere-ionosphere coupling including turbulent transport. J. Geophys. Res. 88, 365-380, 1983

Mallinckrodt, A.J., Carlson, C.W.: Relations between transverse electric fields and field-aligned currents. J. Geophys. Res. 83, 1426–1432, 1978

Pashin, A.B., Glaßmeier, K.H., Baumjohann, W., Raspopov, O.M., Yahnin, A.G., Opgenoorth, H.J., Pellinen, R.J.: Pi 2 magnetic pulsations, auroral break-ups, and the substorm current wedge: a case study. J. Geophys. 51, 223-233, 1982

Pedersen, A., Grard, R., Knott, K., Jones, D., Gonfalone, A.: Measurements of quasi-static electric fields between 3 and

7 earth radii on GEOS-1. Space Sci. Rev. 22, 333-346, 1978

Robert, P., Gendrin, R., Perraut, S., Roux, A., Pedersen, A.: GEOS-2 identification of rapidly moving current structures in the equatorial outer mangetosphere during substorms. J. Geophys. Res. 89, 819-840, 1984

Samson, J.C.: Pi 2 pulsations: high latitude results. Planet.

Space Sci. 30, 1239-1247, 1982

Shepherd, G.G., Boström, R., Derblom, H., Fälthammar, C.-G., Gendrin, R., Kaila, K., Korth, A., Pedersen, A., Pellinen, R., Wrenn, G.: Plasma and field signatures of poleward propagating auroral precipitation observed at the foot of the GEOS-2 field line. J. Geophys. Res. 85, 4587-4601, 1980

Received December 14, 1984; Revised February 28, 1985 Accepted March 28, 1985

Short communication

Velocity-viscosity correlation in convection cells with non-uniform viscosity

U.R. Christensen

Institut für Geowissenschaften, Universität Mainz and Max-Planck-Institut für Chemie*, Saarstraße 23, D-6500 Mainz, Federal Republic of Germany

Abstract. The correlation between the logarithm of local viscosity η and local velocity v (log $|v| \cong a - b \log \eta$) in numerical models of variable viscosity convection is studied. Nineteen selected cases of 2-D stationary convection with different viscosity laws including non-Newtonian rheology, different Rayleigh numbers and different aspect ratios are studied. The quality of correlation is very different, ranging from non-existent to very good. The coefficient b is found to be below 0.5 in almost all cases. Heuristic arguments on the structure of mantle convection which are based on assumptions as $|v| \propto \eta^{-1}$ therefore appear unfounded.

Key words: Convection - Viscosity

Introduction

The rheology of mantle rock is strongly temperature and pressure dependent. Possibly it is also non-Newtonian or stress dependent. Some attempts have been made to determine the influence of non-constant viscosity on the structure of mantle convection by solving the equations of motion and energy transport (e.g. Torrance and Turcotte, 1971; Houston and DeBremaecker, 1975; Schmeling and Jacoby, 1981). However, these efforts have been sporadic and did not attack the problem in a very systematic way. Recently I have studied the heat transport properties of variable viscosity convection in a large number of model cases (Christensen, 1984a, 1985). These models provide the data basis for the present investigation.

The lack of exact systematic solutions for the variable viscosity convection problem has often been bypassed by the use of scaling analysis, heuristic arguments and intuition. For example, it appears reasonable to assume a higher flow velocity v in parts of the convection cell where the viscosity η is lower than in those where η is high. It has been speculated that the thermal state of the mantle may be closer to isoviscous than to adiabatic because the advective heat transport should be less efficient in regions of high viscosity. In order to study this issue by scaling analysis, Fowler (1983) as-

$$|v| \propto \eta^{-1}$$
. (1)

Such a relation, if it could be confirmed, would have important consequences. A viscosity increase by two orders of magnitude from the upper to the lower mantle (Hager, 1984) would reduce the velocity from O(1 cm/year) to O(0.1 mm/year) in the lower mantle. Such low velocity would significantly influence ideas about mixing of mantle heterogeneities and tapping of geochemical 'reservoirs'. Although Eq. (1) may appear intuitively appealing, the arguments to support it are rather weak. Given a certain stress level, it is not the velocity but its spatial derivatives which are related to the viscosity. Furthermore, there is no a priori reason to assume the same level of stress in regions of different viscosity within the cell. In a previous comment to Fowler's paper (Christensen, 1983), I have presented some qualitative arguments as to why I expect the relation between v and η to be much weaker than Eq. (1) assumes. However, it appears useful to determine the correlation between local velocity and local viscosity systematically from numerical solutions of variable viscosity convection.

Results

The finite element solutions which are used to study the correlation are described in more detail elsewhere (Christensen, 1984a, 1985). They are for two-dimensional steady state convection in rectangular boxes. In most case studies the boundaries are stress-free, the temperature difference from top to bottom is fixed and there are no internal heat sources. Besides the aspect ratio l, a Rayleigh number Ra₀ based on the viscosity at the top boundary and two rheological parameters (θ and ζ) describing temperature and pressure dependence determine the state of convection:

$$Ra_0 = \frac{\alpha g \rho \Delta T h^3}{\kappa \eta_0} \tag{2}$$

$$\eta = \eta_0 \exp\left(-\theta \, \bar{T} + \zeta \, \bar{z}\right). \tag{3}$$

 α stands for the coefficient of thermal expansion, g for the gravitational acceleration, ρ for the density, ΔT is

sumed that local velocity and local viscosity correlate like

^{*} Mailing address